

Article

Theoretical Calculations for Highly Selective Direct Heteroarylation Polymerization: New Nitrile-Substituted Dithienyl-Diketopyrrolopyrrole-Based Polymers

Thomas Bura^{1,†}, Serge Beaupré^{1,†}, Marc-André Légaré², Olzhas A. Ibraikulov³ ,
Nicolas Leclerc⁴ and Mario Leclerc^{1,*} 

¹ Canada Research Chair on Electroactive and Photoactive Polymers, Department of Chemistry, Université Laval, Quebec City, QC G1V 0A6, Canada; thomas.bura.1@ulaval.ca (T.B.); serge.beaupre.1@ulaval.ca (S.B.)

² Institut für Anorganische Chemie, Julius-Maximilians Universität Würzburg, Am Hubland, 97074 Würzburg, Germany; marcandrelegare@gmail.com

³ Laboratoire ICube, DESSP, Université de Strasbourg, CNRS, 23 rue du Loess, 67037 Strasbourg, France; ibraikulov@unistra.fr

⁴ Institut de Chimie et Procédés pour l'Énergie, l'Environnement et la Santé, ICPEES, Université de Strasbourg, CNRS, 67087 Strasbourg, France; leclercn@unistra.fr

* Correspondence: Mario.Leclerc@chm.ulaval.ca

† These authors contributed equally to this work.

Academic Editors: Roman Dembinski and Derek J. McPhee

Received: 3 August 2018; Accepted: 11 September 2018; Published: 12 September 2018



Abstract: Direct Heteroarylation Polymerization (DHAP) is becoming a valuable alternative to classical polymerization methods being used to synthesize π -conjugated polymers for organic electronics applications. In previous work, we showed that theoretical calculations on activation energy (E_a) of the C–H bonds were helpful to rationalize and predict the selectivity of the DHAP. For readers' convenience, we have gathered in this work all our previous theoretical calculations on E_a and performed new ones. Those theoretical calculations cover now most of the widely utilized electron-rich and electron-poor moieties studied in organic electronics like dithienyl-diketopyrrolopyrrole (DT-DPP) derivatives. Theoretical calculations reported herein show strong modulation of the E_a of C–H bond on DT-DPP when a bromine atom or strong electron withdrawing groups (such as fluorine or nitrile) are added to the thienyl moiety. Based on those theoretical calculations, new cyanated dithienyl-diketopyrrolopyrrole (CNDT-DPP) monomers and copolymers were prepared by DHAP and their electro-optical properties were compared with their non-fluorinated and fluorinated analogues.

Keywords: DHAP; selectivity; theoretical calculations; conjugated polymers; organic electronics

1. Introduction

Organic solar cells (OSCs) and organic field-effect transistors (OFETs) based on π -conjugated polymers are widely studied to create efficient, lightweight and flexible electronic devices using inexpensive and environmentally friendly printing techniques [1–6]. With power conversion efficiency (PCE) exceeding 10% [7–11] and OFETs with hole mobility up to $20 \text{ cm}^2 \text{ V}^{-1} \text{ s}^{-1}$ [12] and electron mobility as high as $7.0 \text{ cm}^2 \text{ V}^{-1} \text{ s}^{-1}$ [13], conjugated polymers have now reached performances suitable for commercial applications. This is especially true if these materials can be prepared from a low-cost, eco-friendly, reliable and scalable polymerization method such as direct heteroarylation polymerization

(DHAP). Indeed, DHAP is becoming a valuable alternative to classical polymerization methods used in organic electronics. Despite its recent development, this new polymerization method has already been the subject of several comprehensive reviews and book chapters [14–22]. Significant work is underway to understand and limit some unwanted reactions such as β -branching and homocoupling when several C–H bonds can be activated during the polymerization. New catalytic systems [23–25], β -protecting group with no harm on the backbone coplanarity [26] and theoretical calculations on activation energy of C–H bonds [27] are among the actual tools to better understand, limit and eliminate such unwanted reactions.

Among all materials studied in organic electronics, 2,5-dihydropyrrolo[3,4-c]pyrrole-1,4-dione (DPP)-based polymers are on the short list of materials that show high performances in both OSCs (PCE up to 9.4%) [28] and OFETs (hole mobility up to $10.5 \text{ cm}^2 \text{ V}^{-1} \text{ s}^{-1}$) [29]. Since the first report on the synthesis of 3,6-diphenyl-DPP by Farnum et al. in 1974 [30], DPP-based copolymers have been extensively studied and reviewed [31–34]. The flanking aromatic substituents (five- or six-membered-fused or unfused heterocyclic rings) strongly modulate the electro-optical properties. Flanking thiophenes have minimal steric effects on the DPP core and lead to co-planar dithienyl-DPP building blocks (DT-DPP). Recently, we have reported that fluorination of dithienyl-DPP-based monomers (fDT-DPP) is a valuable strategy to obtain well-defined, defect-free DPP-based copolymers by DHAP with enhanced performances in OSCs and OFETs compared to their non-fluorinated analogues [26]. Indeed, a PCE of 7.5% was obtained for fDT-DPP/carbazole copolymer which was twice that of non-fluorinated counterpart. This PCE value is among the highest values reported so far for OSCs based on conjugated polymers obtained by DHAP [35,36].

Besides fluorination, other electron-withdrawing substituent such as nitrile groups have also been used in conjugated polymers to tailor their electronic properties [37–47]. As reported in the literature, cyanation of the conjugated backbone is an efficient strategy to modulate the electro-optical properties of conjugated polymers and in some cases, it can lead to materials with better performances compared to their fluorinated analogues [48]. The nitrile group is a strong electron-withdrawing group that strongly stabilizes the LUMO energy level (without raising the HOMO level) which contributes to reduce the band gap of the resulting copolymers [43,46]. Nitrile groups have also been shown to induce strong dipole moments and promote balanced ambipolar charge transport [49,50]. The main drawback of the cyanation on the conjugated backbone is the lower solubility compared to their non-cyanated analogues which lead to low molecular weight materials with limited processability [42].

In this work, we have summarized all of our theoretical calculations performed on activation energy of the C–H bonds of most of the widely used electron-rich and electron-poor moieties studied in organic electronics. In previous work, we found that the E_a values were helpful to rationalize and predict regio-selectivity of the DHAP when multiple C–H bonds can be activated during the polymerization [26,27]. Based on new theoretical calculations, we then synthesized cyanated dithienyl-Diketopyrrolopyrrole (CNDDT-DPP) derivatives suitable for DHAP. CNDDT-DPP comonomers were then polymerized with either dithienyl-DPP (DT-DPP) or 2,7-dibromocarbazole derivatives and the electro-optical properties of the resulting CNDDT-DPP copolymers were compared with their non-cyanated and fluorinated analogues.

2. Results and Discussion

2.1. Theoretical Calculations

DFT calculations at the B3LYP/TZVP (DZVP for palladium) level have been carried out to evaluate the activation barrier of the C–H bond activation of the Concerted-Metalation Deprotonation (CMD) pathway during DHAP. The model palladium catalyst $(\text{PMe}_3)_2\text{Pd}(\text{Ph})(\text{CH}_3\text{COO}^-)$ was used as a platform to calculate the Gibbs free energy of the CMD transition state associated to the activation of the different C–H bonds of each substrate. The activation energy (E_a , Figures 1 and 2) refers to the Gibbs free energy of the CMD transition state referenced to the substrate and model catalyst (ΔG^\ddagger_{298})

as reported in previous studies [26,27,51,52]. These calculations are relevant to α versus β selectivity of DHAP for possible β -defects but do not say anything about potential α - α homocouplings. From those theoretical calculations, it is also possible to estimate (using Arrhenius's law) a selectivity ratio between H_α and H_β at the temperature of polymerization [26]. More importantly, these calculations reveal the importance of the pairing of the comonomers used in DHAP.

Indeed, the data indicate that the presence of bromine atoms (Figures 1 and 2) decreases the energy of activation (E_a) of the adjacent C–H bonds, allowing undesirable β -defects for some brominated aromatic units. For instance, if we utilized the DHAP with Br-BDT-Me or Br-BDT-OMe and DPP (Figure 1); the difference in the activation energy (ΔE_a) between H_α and H_β for the DPP moiety is found to be $4.8 \text{ kcal}\cdot\text{mol}^{-1}$ (24.2 vs. $29.0 \text{ kcal}\cdot\text{mol}^{-1}$, respectively), which lead to a ratio of about 250:1 favoring H_α (using Arrhenius's law). On the other hand, the E_a of the H_β of the Br-BDT-Me is $28.2 \text{ kcal}\cdot\text{mol}^{-1}$ whereas the E_a for H_β on the Br-BDT-OMe is only $26.7 \text{ kcal}\cdot\text{mol}^{-1}$. Using these values, the ΔE_a between H_α of DPP ($24.2 \text{ kcal}\cdot\text{mol}^{-1}$) and the H_β of the Br-BDT-OMe ($26.7 \text{ kcal}\cdot\text{mol}^{-1}$) and Br-BDT-Me ($28.2 \text{ kcal}\cdot\text{mol}^{-1}$) are respectively of 2.5 and $4.0 \text{ kcal}\cdot\text{mol}^{-1}$, giving respective selectivity of about 25:1 and 160:1 at 125°C . Although the $1.5 \text{ kcal}\cdot\text{mol}^{-1}$ difference might look small, it indicates that the activation of the H_β of the Br-BDT-OMe may occur about one order of magnitude faster than the one of the H_β of the Br-BDT-Me resulting in more β -defects, while the polymer using Br-BDT-Me will better behave in term of selectivity.

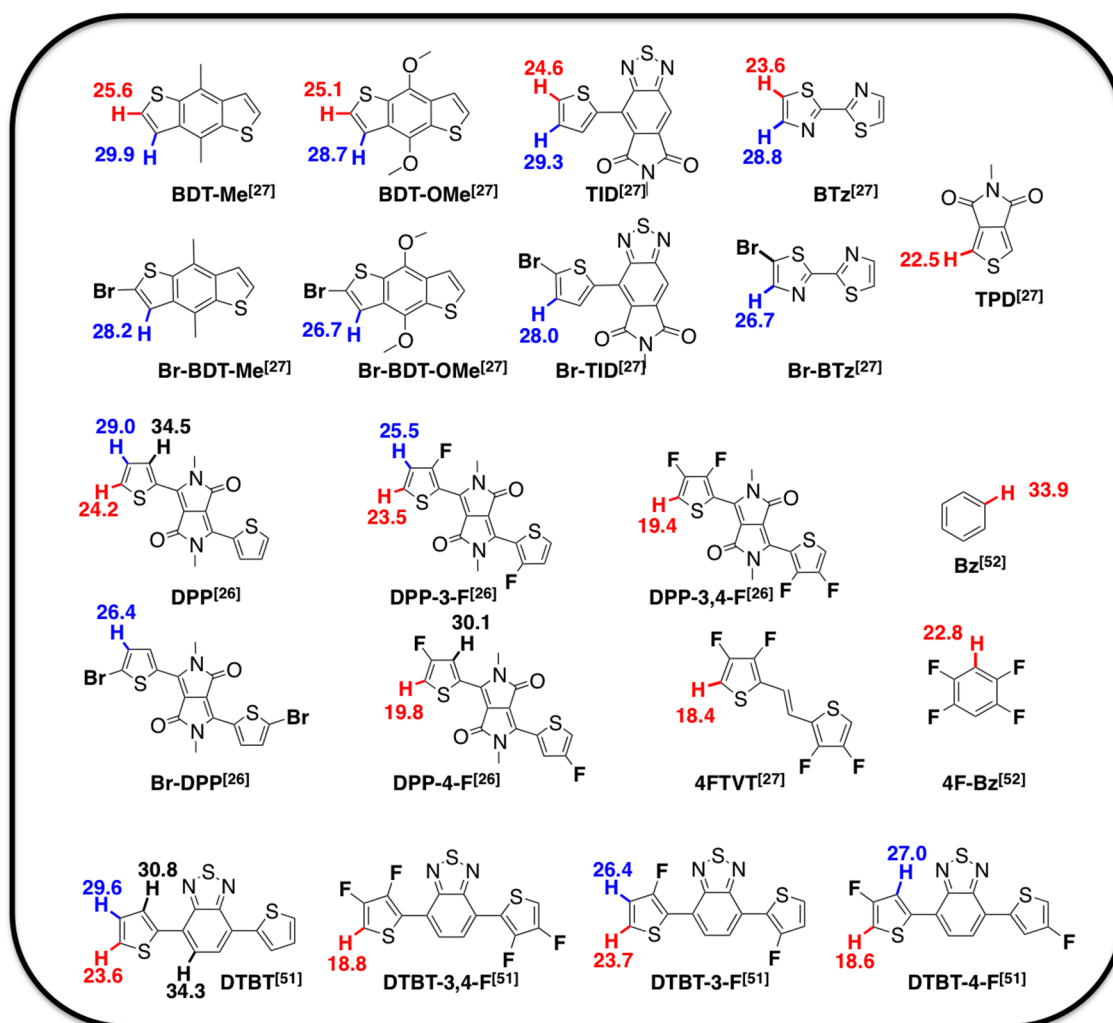


Figure 1. Gibbs free energy of the CMD transition state associated to the transition state for the C–H bond cleavage (previous work: [26,27,51,52]).

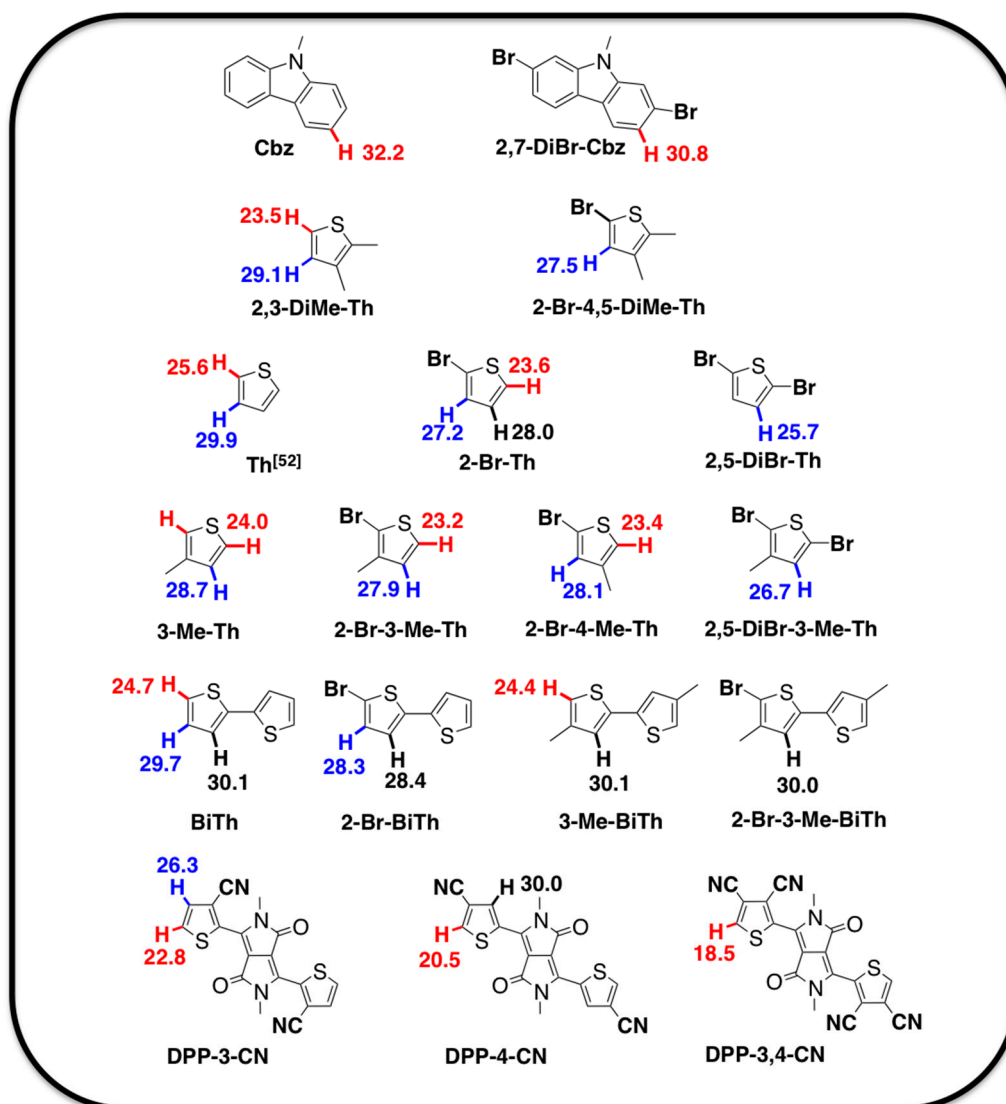


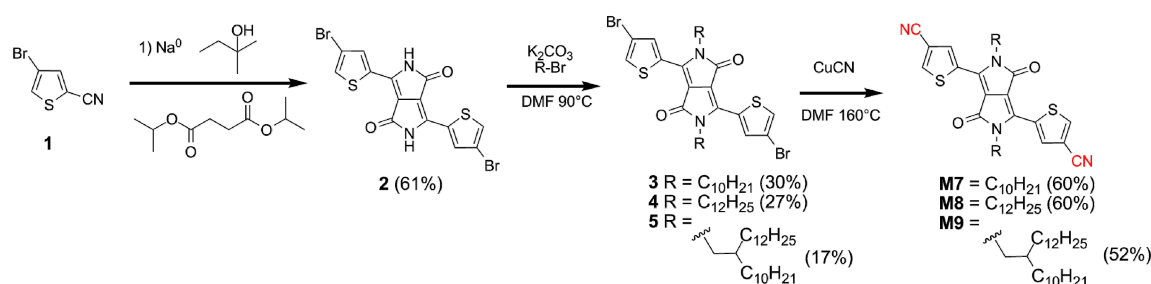
Figure 2. Gibbs free energy of the CMD transition state associated to the transition state for the C–H bond cleavage (this work [52]).

These calculations indicate that some brominated monomers are not intrinsically inadequate but their utilization is strongly dependent upon the nature and reactivity of the respective comonomer. This has been proven by the work of Li et al. [53]. Indeed, well-defined copolymer was obtained from the copolymerization of Br-DPP with bithiazole (BTz) while poor performances were obtained for the same copolymer synthesized using Br-BTz and DPP. For the first case, the ΔE_a between the H_α (23.6 kcal·mol⁻¹) and H_β (28.8 kcal·mol⁻¹) of BTz is 5.2 kcal·mol⁻¹ which means that the activation of the H_α position is highly selective (ratio 1152:1). Meanwhile, a selectivity of about 35:1 is observed when considering the ΔE_a value of 2.8 kcal·mol⁻¹ between H_β of the Br-DPP (26.4 kcal·mol⁻¹) and H_α of the BTz (23.6 kcal·mol⁻¹). On the other hand, for the Br-BTz/DPP system, the ΔE_a between H_β of the Br-BTz (26.7 kcal·mol⁻¹) and the H_α of the DPP (24.2 kcal·mol⁻¹) is 2.5 kcal·mol⁻¹ (ratio 23:1) and should lead to less-defined structure.

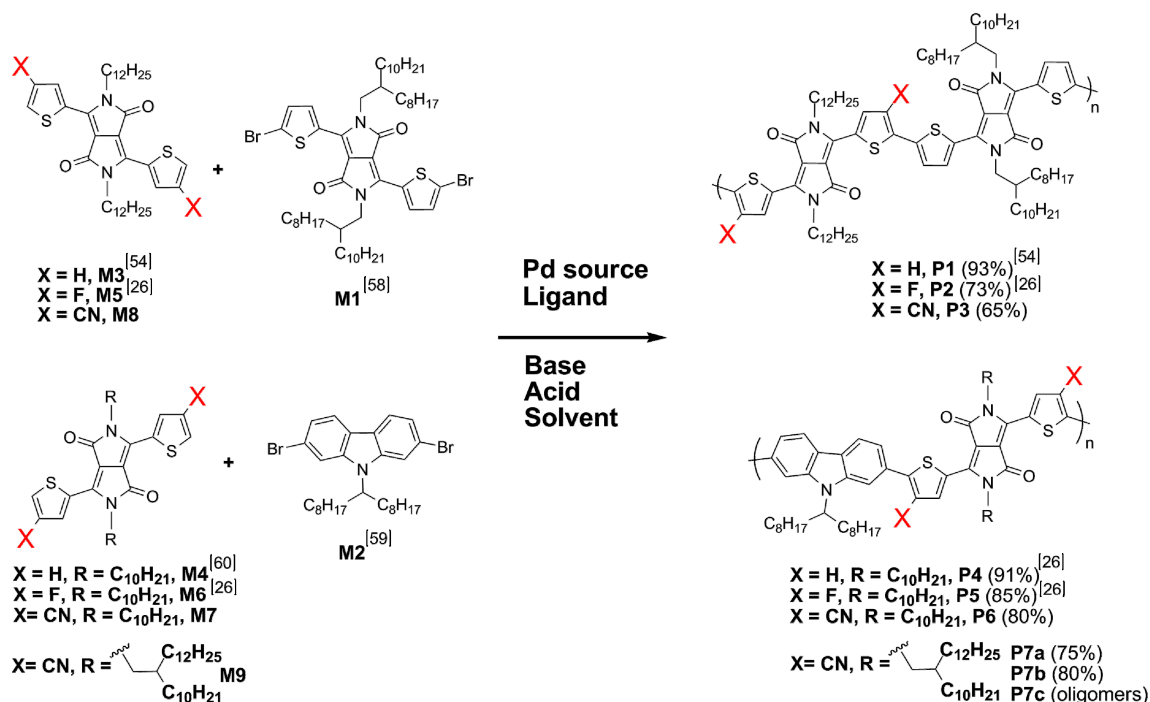
2.2. Justification for Cyano-Dithienyl-DPP (CNDT-DPP)

Lately, we have shown that the fluorination of flanking thiophene (at the 3- or 4-position) influences the electro-optical properties and the coplanarity of the DPP-based copolymers and to obtain a coplanar fluorinated DPP, the fluorine atom has to be installed at the 4-position of

thiophene ring [26,51]. A fluorine atom at the 4-position on flanking thiophene strongly decreases the activation energy of the adjacent C–H bond (from 24.2 kcal·mol⁻¹ to 19.8 kcal·mol⁻¹) for DPP moiety (Figure 1). We then performed a similar study by replacing the fluorine atom by a nitrile group, a strong electron-withdrawing moiety. As shown in Figure 2, the nitrile groups have also a strong influence on the adjacent C–H bonds. Indeed, we found a ΔE_a of 3.7 kcal·mol⁻¹ for H_α of DPP-4-CN (20.5 kcal·mol⁻¹) vs DPP (24.2 kcal·mol⁻¹) and 4.5 kcal·mol⁻¹ for H_γ of DPP-4-CN (30.0 kcal·mol⁻¹) vs. DPP (34.5 kcal·mol⁻¹). Although, the activation energy of H_γ is decreased by 4.5 kcal·mol⁻¹ compared to DPP, a selectivity of about 500,000/1 in favor of H_α over H_γ was calculated using Arrhenius's law. This means that polymerization reaction should mainly occur at the α-position and lead to well-defined materials. The same trend was observed for DPP-3-CN vs. DPP-3-F and DPP-3,4-CN vs. DPP-3,4-F. Keeping in mind the need for coplanar copolymers, only DPP-4-CN was synthesized (Scheme 1) and copolymerized by DHAP (Scheme 2).



Scheme 1. Synthetic Pathway for the Synthesis of CN-DPP Comonomers M7, M8 and M9.



Scheme 2. Monomers and Polymers Investigated in this Work. [26,54–57].

2.3. Synthesis of Monomers

A pseudo Stobbe condensation between diisopropyl succinic ester and commercially available 4-bromothiophene-2-carbonitrile (1) in the presence of sodium alkoxide led to 3,6-(4-bromo-thiophen-2-yl)pyrrolo[3,4-c]pyrrole-1,4-dione (2) in moderate yield (61%, Scheme 1). In the next step, a typical alkylation reaction of the DPP core was performed using either 1-bromodecane, 1-bromododecane or 1-bromo-2-decyltetradecane and allowed us to obtain

corresponding alkylated DPP 3–5 in low yields (17–30%). Finally, the target monomers **M7–M9** (see Supplementary Materials) were obtained in good yield by cyanation of the respective brominated DPP through a Rosenmund-von Braun cyano-dehalogenation reaction with CuCN in hot anhydrous DMF as described in the literature [49]. For comparison purposes, **M7–M9** were obtained in three steps with an overall yield of 10% while **M5** and **M6** (fDT-DPP analogues) [26] were obtained in seven steps with an overall yield of 8%.

2.4. Synthesis and Characterization of Polymers

P3, **P6** and **P7** were prepared by direct (hetero)arylation polymerization (DHAP) following methodologies previously reported in the literature (Scheme 2) [26]. Cyanated dithienyl-DPP (CNDT-DPP) pseudo-homopolymer **P3** was synthesized for future OFETs applications while CNDT-DPP/carbazole copolymers **P6**, **P7** were designed to be used as an electron-donor in OSCs. According to theoretical calculations, the reaction between Br-DPP **M1** and DPP-4-CN **M8** (Figures 1 and 2) should proceed smoothly without β -branching on the DPP-4-CN or on the Br-DPP moieties. Indeed, the β -position is protected by the nitrile group on the DPP-4-CN and the H_{α} has an E_a of 20.5 kcal·mol⁻¹ while the E_a of H_{β} on the Br-DPP is 26.4 kcal·mol⁻¹. The ΔE_a between H_{β} of Br-DPP (26.4 kcal·mol⁻¹) and the H_{α} of DPP-4-CN (20.5 kcal·mol⁻¹) is 5.9 kcal·mol⁻¹ which lead to an estimated selectivity of 1800:1 in favor of the H_{α} of the DPP-4-CN. The same reasoning should also apply for **P6** involving the reaction between **M2** (Scheme 2) and **M7** (Figure 2). The β -position on DPP-4-CN is protected by the nitrile group and the ΔE_a between H_{α} of DPP-4-CN (20.5 kcal mol⁻¹) and the H_{α} of Br-Cbz (30.8 kcal·mol⁻¹) is 10.3 kcal·mol⁻¹ which lead to an estimated selectivity of 687,000:1 in favor of the H_{α} of DPP-4-CN. It is worth nothing that **P3** and **P6** were synthesized using the same catalytic conditions as those used for their fluorinated analogues [26]. Unlike fDT-DPP based copolymers **P2** [26], the polymerization reaction of **P3** was stopped rapidly (10 min) due to gelation of the reaction mixture.

As shown in Table 1, the polymerization time for **P3** (10 min) and **P6** (40 min) were shorter compared to the polymerization times of DT-DPP analogues (1200 min for **P1** and 960 min for **P4**). As for fDT-DPP comonomers, the shorter polymerization times compared to those observed for the non-fluorinated are due to strong electron-withdrawing effect of the cyano group on the α C–H bond. Moreover, the polymerization times for **P6** vs **P5** were similar which might mean that the reactivity of **M7** and **M6** are similar, which is in good agreement with the E_a of DPP-4-CN (20.5 kcal·mol⁻¹) vs. E_a of DPP-4-F (19.8 kcal·mol⁻¹). Unlike **P2**, we were unable to determine the molecular weights of **P3** due to strong aggregation and limited solubility, even in TCB at 135 °C. On the other hand, the molecular weight of **P6** (soluble fraction) was lower compared to **P4** and **P5**. The short polymerization time (40 min), due to rapid gelation of the reaction mixture, led to a material with low molecular weight. In the hope of promoting the solubility of CNDT-DPP/Carbazole copolymers, long and branched alkyl side chains were installed on the CNDT-DPP moiety (see **M9** in Scheme 1). **P7a** was obtained by DHAP from **M2** and **M9** using the same catalytic system used for the synthesis of **P6** but in more dilute conditions in superheated tetrahydrofuran ($C = 0.085$ mol·L⁻¹ for **P7a** vs. $C = 0.1$ mol·L⁻¹ for **P6**). Despite a longer polymerization time before gelation of the reaction mixture happened for **P7a** (240 min), a lower molecular weight material was obtained. **P7b** was then synthesized using the same polymerization conditions used for **P6** ($C = 0.1$ mol·L⁻¹ in THF). As for **P6**, gelation of the polymerization mixture was observed after only 40 min. Despite higher \overline{M}_n (35 kg mol⁻¹) the degree of polymerization of **P7b** and **P6** are the same (DP = 24). Finally, **P7c** was synthesized using chlorobenzene instead of THF ($C = 0.1$ mol·L⁻¹) but the polymerization did not work and only oligomers were recovered. **P6** was then used for comparison purposes with **P4** and **P5** since these polymers have the same side chains installed on the DPP moiety.

Table 1. Characterization of P1–P7a–c.

	\overline{M}_n	\mathcal{D}	Yield	Reaction Time	T_d
	kg mol ⁻¹		%	min	°C
P1 [54]	16	2.4	93	1200	n.a
P2 [26]	22	3.0	73	1200	430
P3	n.a.	n.a.	65	10	420
P4 [26]	44	3.0	91	960	420
P5 [26]	125	3.0	85	30	420
P6	25	3.5	80	40	405
P7a	20	1.7	75	240	405
P7b	35	2.4	80	40	410
P7c	oligomers			-	-

\overline{M}_n : number-average molecular weight; \mathcal{D} : Dispersity Index.

Thermal properties were evaluated by thermogravimetric analysis (TGA) and differential scanning calorimetry (DSC). All polymers exhibit good thermal stability with 5% weight loss at temperature higher than 400 °C (see Table 1). Differential scanning calorimetry measurements did not reveal any thermal transition. NMR spectroscopy was useless to identify any defect within the conjugated backbone for P3 and P6 due to broad and featureless signals.

The UV-Vis-NIR absorption spectroscopy (solution and film) was performed to gauge the effect of substituents at 4-position on flanking thiophene DPP core on the optical properties and the results are summarized in Table 2. The absorption spectra of P1–P6 are shown in Figures 3 and 4. In dilute chloroform solution, a bathochromic shift of the maximum of absorption (19 nm) was observed for P6 (674 nm) compared to P4 (655 nm). In the same condition, a hypsochromic shift of 28 nm was observed for the maximum of absorption of P6 (674 nm) compared to the maximum of absorption of P5 (702 nm). Beside the fact that \overline{M}_n of P5 (125 kg mol⁻¹) is much higher than P6 (25 kg mol⁻¹), the optical band gaps were found to be almost identical (1.68 eV for P6 and 1.65 eV for P5). The hypsochromic shift observed for P6 is due to a conformational twisting of the conjugated backbone due to the larger size of the nitrile group compared to fluorine which was confirmed by conformational analyses performed on the repeating unit of P5 and P6 (Figure 5). The calculations suggest that P6 is more twisted than P5 (30.6° vs. 24.0°), which should reduce the effective length of conjugation of the polymer.

Table 2. Electro-optical properties of P1–P6.

	HOMO ^a	LUMO ^a	E_g^{cv}	LUMO ^b	λ_{max}		E_g^{opt}
					Solution	Film	
					eV	eV	
P1 [54]	-5.13	-3.82	1.31	-3.96	820/920	846/927	1.17
P2 [26]	-5.35	-3.69	1.66	-4.20	887/962	859/967	1.15
P3	-5.44	-3.96	1.48	-4.28	907	881	1.16
P4 [26]	-5.11	-3.46	1.65	-3.43	622/655	630/689	1.68
P5 [26]	-5.33	-3.61	1.72	-3.68	639/702	639/702	1.65
P6	-5.54	-3.79	1.75	-3.86	621/674	620/676	1.68
P7a	-5.54	-3.79	1.75	-3.86	620/673	621/674	1.73
P7b	-5.54	-3.79	1.75	-3.86	621/674	621/676	1.72

^a from CV measurements. ^b $E_{LUMO} = E_{HOMO} + E_g^{opt}$.

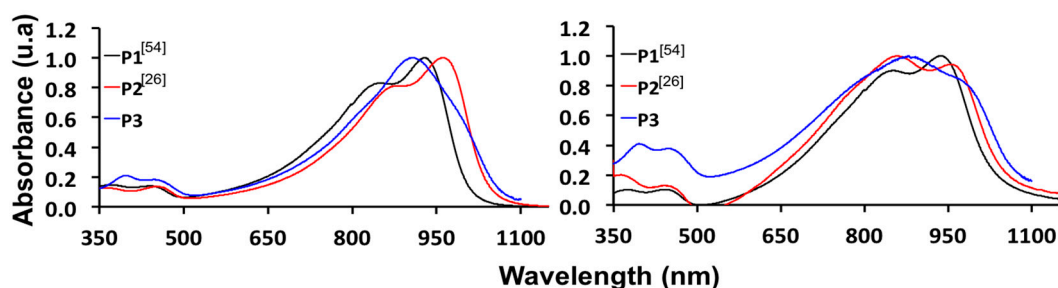


Figure 3. UV-Visible absorption spectra of P1–P3 in solution in CHCl_3 (left) and in the solid state (right) [26,54].

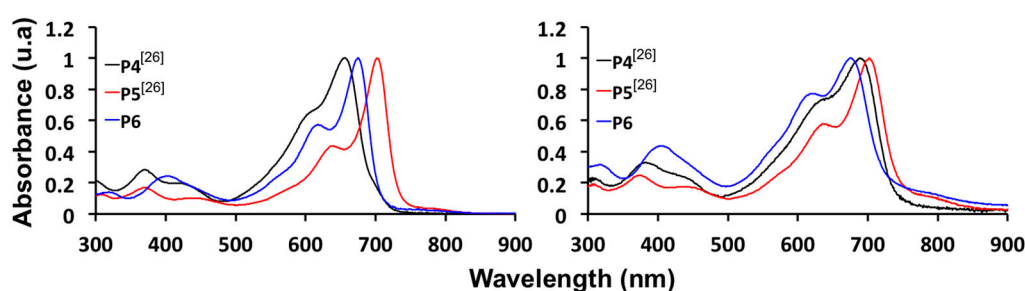


Figure 4. UV-Visible absorption spectra of P4–P6 in solution in CHCl_3 (left) and in the solid state (right) [26].

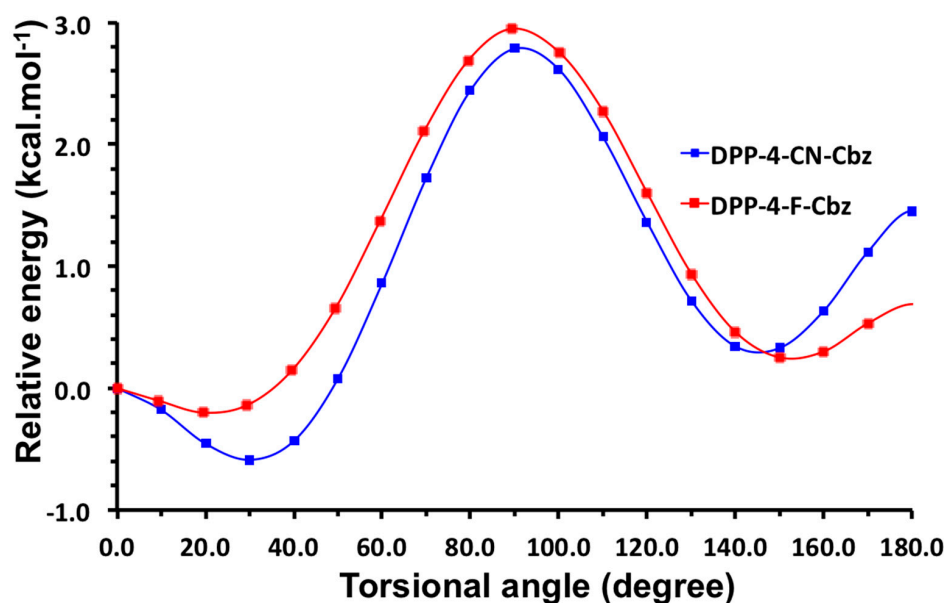


Figure 5. Ground-state energy surfaces of CBz-DPP-4-F and CBz-DPP-4-CN dimers.

Electrochemical measurements such as cyclic voltammetry are a widely used method in organic electronics to estimate the HOMO and LUMO energy levels analyses. In order to be able to compare the values reported in literature, it is of the utmost importance that the measurements are performed under the same conditions (electrolyte, working electrode, reference electrode (non-aqueous is highly desirable), scanning speed, determination of the onset oxidation and reduction, and calibration against Ferrocene). Comparisons between datasets can be therefore misleading. Lately, we found that some HOMO/LUMO values reported might have been over-estimated. This issue has been fixed and the HOMO/LUMO values reported in Table 2 reflects those changes. As example, we have previously reported for P1 a HOMO energy level of -5.45 eV and a LUMO energy level of -4.14 eV [54]. After corrections the HOMO and LUMO energy levels are now -5.13 eV and -3.82 eV, which is in

good agreement with DPP-based polymers reported in literature [33]. The same corrections have been done for **P2** and **P5** previously reported in literature [26]. For **P1–P3**, a stabilization of the HOMO energy level was observed upon fluorination and cyanation of the DPP moiety (Figure 6).

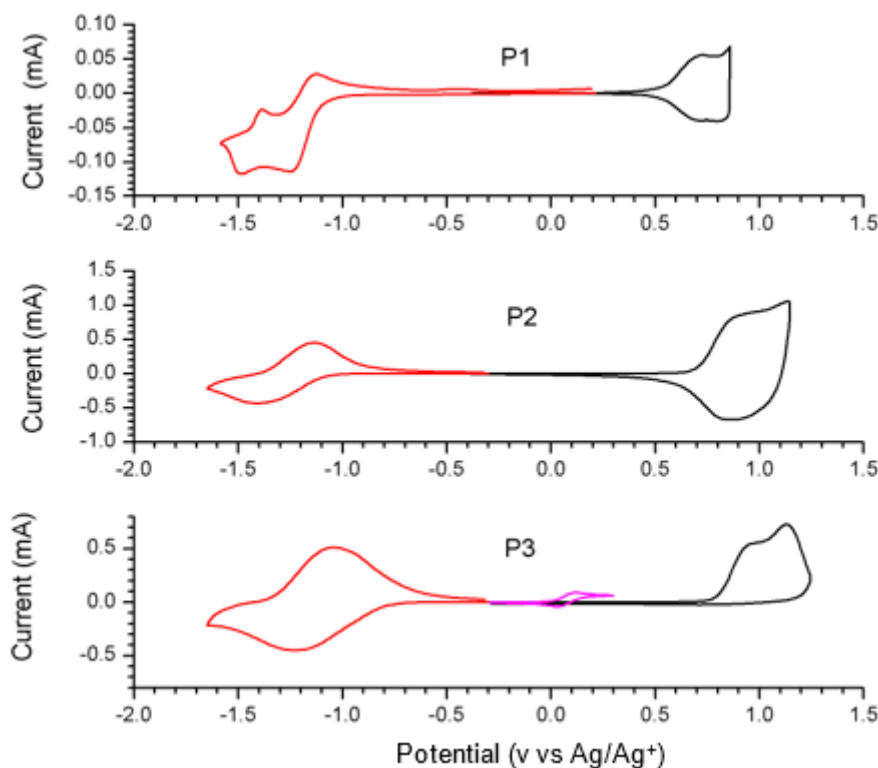


Figure 6. Cyclic voltammetry of **P1** [54], **P2** [26] and **P3** (In magenta, Fc/Fc+).

Indeed, the HOMO level of **P2** (−5.35 eV) was stabilized by 0.22 eV while the HOMO level of **P3** (−5.44 eV) was stabilized by 0.31 eV compared to HOMO level of **P1** (−5.13 eV). The same trend was observed for **P4–P6** (Figure 7). The stabilization of the HOMO level due to cyanation of DPP moiety was even larger for **P6** (0.43 eV). These data are in good agreement with the trend observed for the cyanation of conjugated polymers. It is worth nothing that deeper HOMO energy levels might lead to a higher open circuit voltage (V_{oc}) in OSCs. On the other hand, the LUMO energy levels were also determined from cyclic voltammetry even though reduction measurements are more sensitive to water and oxygen. While the estimated LUMO energy levels obtained by cyclic voltammetry for **P4–P6** (Figure 8) led to E_g^{cv} similar to E_g^{opt} , it was not the case for the **P1–P3** (Figure 6). Indeed, even if reversible reduction processes were observed for each polymer, the band gap (calculated from the reduction and the oxidation onsets) led to E_g^{cv} values that did not match the optical band gap calculated from solid state UV-Vis absorption spectra (Table 2). We found a ΔE_g between E_g^{cv} and E_g^{opt} of 0.14 eV, 0.51 eV and 0.32 eV for **P1**, **P2** and **P3** respectively. Even if stabilization of the LUMO energy levels was observed upon cyanation of the DT-DPP moiety (−3.82 eV to −3.96 eV, Figure 6), it appears that the reduction processes observed for **P1** to **P3** might not correspond to the extraction of electron from the conjugated skeleton but may come from the reduction of other functional group found on the DPP moiety. As reported in literature, the discrepancy between the electrochemical and optical band gaps may also be ascribed to the strong exciton binding energy in conjugated polymers. This binding energy can be as high as 0.4–1.0 eV [58–60]. We then calculated the LUMO energy levels using the optical band gap and the HOMO energy levels (Table 2). Going from **P1** to **P3**, we noticed a steady stabilization of the LUMO energy levels −3.96 eV, −4.20 eV and −4.28 eV. These deep LUMO energy levels make **P2** and **P3** good candidates for *n*-type materials for OFETs or good electron-acceptor in all

polymer solar cells (PSCs). **P3** and **P6** are currently tested in OFETs and PSCs and those results will be reported in a forthcoming paper.

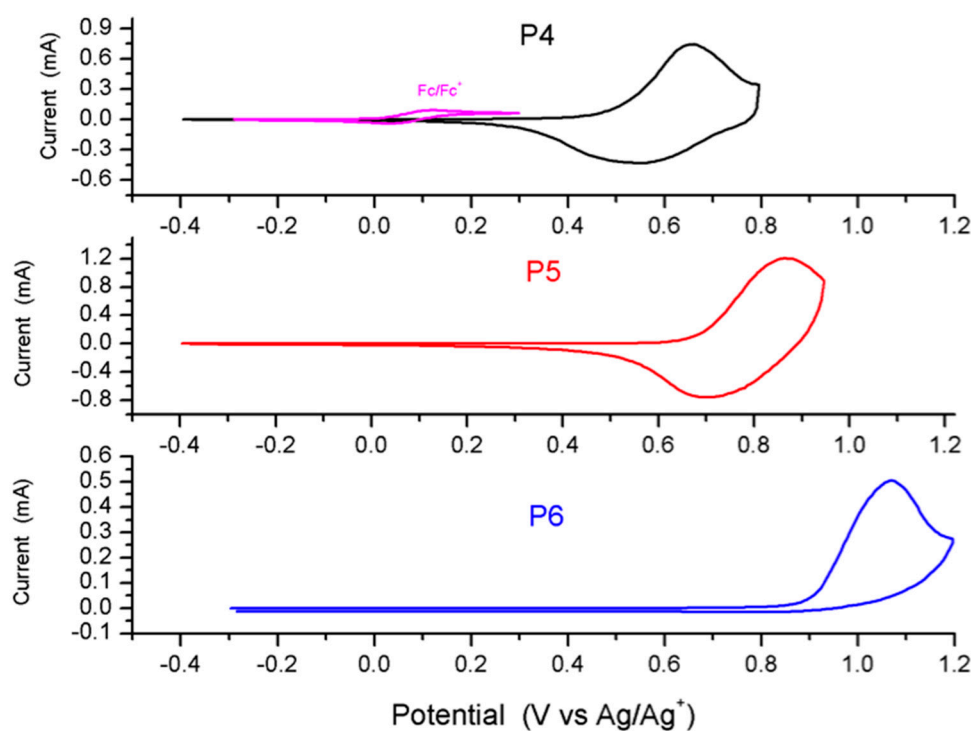


Figure 7. Cyclic voltammetry of P4 [26], P5 [26] and P6.

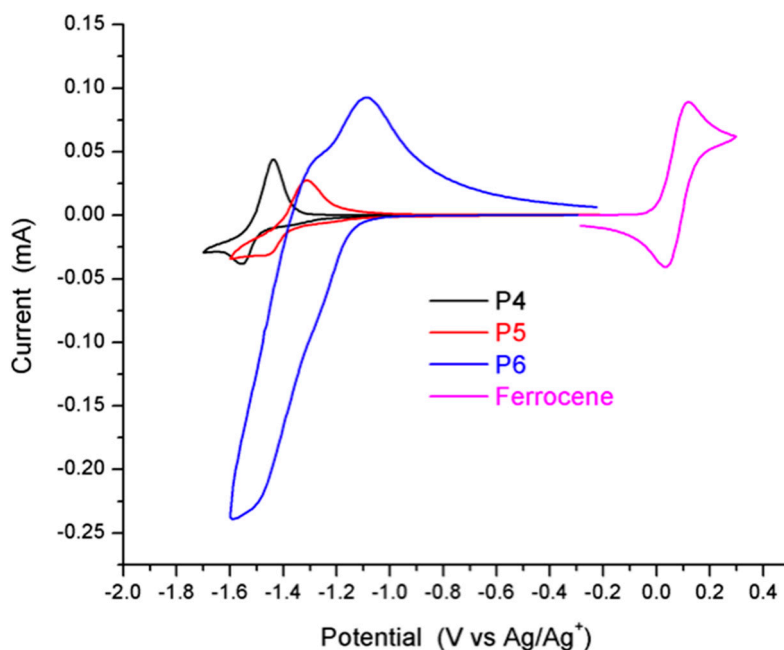


Figure 8. Cyclic voltammetry of P4 [26], P5 [26] and P6 (Reduction only).

3. Materials and Methods

^1H and ^{13}C -NMR spectra were recorded on a Varian AS400 or Agilent DD2 500 MHz apparatus (Santa Clara, CA, USA) in deuterated solvents. Chemical shifts were reported as δ values (ppm) relative to the residual protic solvent (see Supplementary Materials). Infrared Spectra were obtained using a Specac spectrometer using golden gate single reflection attenuated total reflection system

(Pleasantville, NY, USA) fitted with a diamond crystal. The infrared spectra were recorded in solid state with a Nicolet Magna 550 Fourier transform spectrometer (Madison, WI, USA) equipped with a narrow band mercury-cadmium-telluride (MCT) detector and a germanium-coated KBr beam splitter. A total of 64 interferograms were acquired, co-added and Fourier transformed to give a spectral resolution of 4 cm^{-1} in the spectral range of $4000\text{--}800\text{ cm}^{-1}$. High resolution mass spectra were recorded with a time-of-flight spectrometer in flow infusion analysis on an Agilent Technologies 1200 series system (Santa Clara, CA, USA). Ions were generated by a Kr UV lamp in an APPI source with toluene/anisole mixture as dopant when required. Spectra ranging from 100 to 3200 m/z were recorded with typical resolution of 5000 to 15,000 and typical precision of ± 1 ppm or less. The mass analyzer was calibrated with standard solutions provided by the manufacturer and covering the spectral range described above. The number-average (\overline{M}_n) and weight-average (\overline{M}_w) molecular weights were determined by size exclusion chromatography (SEC) using a Varian Polymer Laboratories PL-GPC 120 (Church Stretton, Shropshire, United Kingdom). The column set consists of 2 PL gel Mixed C ($300 \times 7.5\text{ mm}$) columns and a PL gel Mixed C guard column. The flow rate was fixed at 1 mL/min using 1,2,4-trichlorobenzene (TCB) (with 0.0125% BHT w/v) as eluent. The temperature of the system was set to $110\text{ }^\circ\text{C}$. All the samples were prepared at concentrations of nominally 1.0 mg/mL in TCB. Dissolution was performed using a Varian Polymer Laboratories PL-AS RT autosampler. The sample vials were held at $110\text{ }^\circ\text{C}$ with shaking for 1 h for complete dissolution. The solutions were filtered through a 2 mm porous stainless steel filter used with the $0.40\text{ }\mu\text{m}$ glass filter into a 2 mL chromatography vial. The calibration method used to generate the reported data was the classical polystyrene method using polystyrene narrow standards Easi-Vials PS-M from Varian Polymer Laboratories which were dissolved in TCB. UV-Vis absorption spectra were taken using a Thermo Scientific Genesys 10S spectrophotometer (Madison, WI, USA) using 1 cm path-length quartz cells. For solid state measurements, polymer solution was spun-cast on glass plates. Optical bandgaps were calculated from the onset of the absorption band. Thermogravimetric analysis (TGA) measurements were carried out with a Mettler Toledo TGA SDTA 851e apparatus (Columbus, OH, USA) at a heating rate of $10\text{ }^\circ\text{C}/\text{min}$ under a nitrogen atmosphere. The temperature of degradation (T_d) corresponds to a 5% weight loss. Differential scanning calorimetry (DSC) analysis was performed on a Mettler Toledo DSC823e apparatus (Columbus, OH, USA) calibrated with ultrapure indium at a scanning rate of $10\text{ }^\circ\text{C}/\text{min}$ under a nitrogen flow. Cyclic voltammograms were recorded on a Solartron 1287 potentiostat (Oak Ridge, TN, USA) using platinum wires as working electrode and counter electrode at a scan rate of 50 mV/s. The reference electrode was Ag/Ag⁺ (0.01 M AgNO₃ in acetonitrile), and the electrolyte was a solution of 0.1 M tetrabutylammonium tetrafluoroborate (Bu₄NBF₄) in dry acetonitrile. In these conditions, the half-wave oxidation potential of ferrocene was 0.091 V versus Ag/Ag + ($E_{\text{Ferrocene vs. Ag/Ag}^+}^{1/2}$). The HOMO and LUMO energy levels were determined from the oxidation and reduction onsets (E') (where the current differs from the baseline) using the following equations:

$$E_{\text{HOMO}} = -[(E'_{\text{ox vs. Ag/Ag}^+}) + 4.8 - (E_{\text{Ferrocene vs. Ag/Ag}^+}^{1/2})]$$

$$E_{\text{LUMO}} = -[(E'_{\text{red vs. Ag/Ag}^+}) + 4.8 - (E_{\text{Ferrocene vs. Ag/Ag}^+}^{1/2})]$$

3.1. Materials

4-Bromothiophene-2-carbonitrile (**1**) was purchased from Combiblocks (San Diego, CA, USA). **P1** [54], **P2** [26], **P4** [26], **P5** [26], 3,6-bis(5-bromothiophen-2-yl)-2,5-bis(2-octyl-dodecyl)pyrrolo[3,4-c]pyrrole-1,4-dione (**M1**) [55], 2,7-dibromo-9-(heptadecan-9-yl)-9H-carbazole (**M2**) [56], 3,6-bis(thiophen-2-yl)-2,5-bis(dodecyl)pyrrolo[3,4-c]pyrrole-1,4-dione (**M3**) [54], 3,6-bis-(thiophen-2-yl)-2,5-bis(decyl)-pyrrolo[3,4-c]pyrrole-1,4-dione (**M4**) [57], 3,6-(4-fluorothiophen-2-yl)-2,5-Bis(dodecyl)pyrrolo[3,4-c]pyrrole-1,4-dione (**M5**) [26], 3,6-(4-fluorothiophen-2-yl)-2,5-Bis(decyl)pyrrolo[3,4-c]pyrrole-1,4-dione (**M6**) [26] and 4-tris(2-cycloheptyloxyphenyl)phosphine (Bura-Phos) [27] were synthesized according to literature.

3.2. Synthesis of Monomers and Polymers

3.2.1. Synthesis of 3,6-(4-Bromothiophen-2-yl)pyrrolo[3,4-c]pyrrole-1,4-dione (2)

In a two-neck flask equipped with a condenser and an addition funnel, sodium (3.67 g, 0.159 mol, 1.2 eq.) was added in 2-methyl-2-butanol (250 mL), and the mixture was heated at 105 °C until complete consumption of the sodium. Then, 4-bromo-2-thiophenecarbonitrile (1, 25 g, 0.133 mol, 1 eq.) was rapidly added into the mixture, and diisopropyl succinate (12.1 g, 59.8 mmol, 0.45 eq.) was slowly added through the addition funnel. The reaction mixture quickly turned purple. The reaction mixture was stirred overnight at 105 °C. The reaction was cooled at 65 °C and quenched by an addition of a mixture of methanol (150 mL) and acetic acid (70 mL) followed by heating at 90 °C for 30 min. Then, the reaction mixture was allowed to cool to room temperature, filtered on a Buchner, and washed with methanol to give a purple solid (Y = 61%).

3.2.2. Synthesis of 3,6-(4-Bromothiophen-2-yl)-2,5-bis(decyl)-pyrrolo[3,4-c]pyrrole-1,4-dione (3)

In a two-neck flask equipped with a condenser and an addition funnel, compound 2 (1.150 g, 2.51 mmol, 1 eq.) and anhydrous potassium carbonate (1.1 g, 7.53 mmol, 3 eq.) were stirred in anhydrous DMF (8 mL). The mixture was heated at 100 °C for 30 min, and then 1-bromodecane (1.7 g, 7.53 mmol, 3 eq.) was slowly added. The reaction mixture was stirred overnight at 100 °C. After cooling to room temperature, the reaction was quenched with a saturated solution of NH₄Cl and extracted three times with diethyl ether. The combined organic phases were washed with water and brine, dried over MgSO₄, and concentrated under vacuum. Purification was achieved by column chromatography (silica gel; eluent: chloroform/hexanes 85/15) affording the desired compound as a purple solid (Y = 30%). ¹H-NMR (500 MHz, CDCl₃) δ (ppm): 8.81 (s, 2H), 7.52 (s, 2H), 4.02–3.99 (m, 4H), 1.73–1.70 (m, 4H), 1.42–1.26 (m, 28H), 0.90–0.87 (m, 6H). ¹³C-NMR (126 MHz, CDCl₃) δ (ppm): 169.9, 138.8, 136.7, 130.5, 127.7, 112.3, 108.2, 42.3, 31.9, 29.9, 29.6, 29.5, 29.3, 29.2, 26.8, 22.6, 14.1. m.p. = 126 °C. FTIR ν (cm⁻¹) = 3094, 2951, 2916, 2850, 1666, 1576, 1407, 883. HRMS (APPI+): *m/z* calcd for C₃₄H₄₇Br₂N₂O₂S₂: 737.1446; found: 737.1475 [M + H]⁺

3.2.3. Synthesis of 3,6-(4-Bromo-thiophen-2-yl)-2,5-bis(dodecyl)-pyrrolo[3,4-c]pyrrole-1,4-dione (4)

Compound 4 was synthesized and purified according to the procedure described for compound 3 using 1-bromododecane instead of 1-bromodecane affording the desired compound as a purple solid (Y = 27%). ¹H-NMR (500 MHz, CDCl₃) δ (ppm): 8.81 (s, 2H), 7.52 (s, 2H), 4.02–3.99 (m, 4H), 1.73–1.70 (m, 4H), 1.42–1.26 (m, 36H), 0.90–0.87 (m, 6H). ¹³C-NMR (126 MHz, CDCl₃) δ (ppm): 169.9, 138.8, 136.7, 130.5, 127.7, 112.3, 108.2, 42.3, 31.9, 29.9, 29.6, 29.56, 29.52, 29.3, 29.2, 26.8, 22.6, 14.1. m.p. = 132 °C. FTIR ν (cm⁻¹) = 3102, 2917, 2850, 1670, 1557, 1412, 876. HRMS (APPI+): *m/z* calcd for C₃₈H₅₅Br₂N₂O₂S₂: 793.2072; found: 793.2083 [M + H]⁺

3.2.4. Synthesis of 3,6-(4-Bromo-thiophen-2-yl)-2,5-di(2'-decyltetradecyl)-pyrrolo[3,4-c]pyrrole-1,4-dione (5)

Compound 5 was synthesized and purified according to the procedure described for compound 3 using 1-bromo-2-decyltetradecane instead of 1-bromodecane affording the desired compound as a purple solid (Y = 17%). ¹H-NMR (400 MHz, CDCl₃) δ (ppm): 8.69 (d, *J* = 1.4 Hz, 2H), 7.50 (d, *J* = 1.4 Hz, 2H), 3.95 (d, *J* = 7.7 Hz, 4H), 1.85 (m, 2H), 1.27–1.21 (m, 80H), 0.89–0.85 (m, 12H). ¹³C-NMR (101 MHz, CDCl₃) δ (ppm): 161.3, 139.2, 136.4, 130.6, 127.5, 112.1, 108.1, 46.2, 30.0, 29.7, 29.6, 29.5, 29.4, 29.3, 29.2, 22.7, 14.1. HRMS (APPI+): *m/z* calcd for C₆₂H₁₀₃Br₂N₂O₂S₂: 1129.5828; found: 1129.5838 [M + H]⁺

3.2.5. Synthesis of 3,6-(4-Cyano-thiophen-2-yl)-2,5-bis(decyl)-pyrrolo[3,4-c]pyrrole-1,4-dione (M7)

In a microwave vial containing compound 3 (230 mg, 0.311 mmol 1 eq.) and copper(I)cyanide (223 mg, 2.49 mmol, 8 eq.) was added dry DMF (3 mL, C = 0.75 mol·L⁻¹). The mixture was heated under argon for 24 h at 160 °C. The reaction mixture was allowed to cool down to room temperature

and water was added and the crude was extracted three times with diethyl ether. The aqueous phase was extracted three times with diethyl ether. The solvent was removed under reduced pressure and the residue was purified by column chromatography (chloroform/ethyl acetate, 95/5) affording the desired compound as a purple solid (Y = 60%) $^1\text{H-NMR}$ (500 MHz, CDCl_3) δ (ppm): 8.99 (s, 2H), 8.17 (s, 2H), 4.03–4.01 (m, 4H), 1.72–1.69 (m, 4H), 1.42–1.26 (m, 28H), 0.89–0.86 (m, 6H). $^{13}\text{C-NMR}$ (126 MHz, CDCl_3) δ (ppm): 160.7, 138.7, 138.3, 135.2, 131.1, 113.9, 112.5, 108.8, 42.3, 31.8, 30.1, 29.5, 29.3, 29.2, 26.8, 22.6, 14.1. m.p. = 216 °C. FTIR ν (cm^{-1}) = 3081, 2914, 2846, 2233, 1667, 1559, 883. HRMS (APPI+): m/z calcd for $\text{C}_{36}\text{H}_{47}\text{N}_4\text{O}_2\text{S}_2$: 631.3140; found: 631.3177 $[\text{M} + \text{H}]^+$.

3.2.6. Synthesis of 3,6-(4-Cyano-thiophen-2-yl)-2,5-bis(dodecyl)-pyrrolo[3,4-c]pyrrole-1,4-dione (**M8**)

M8 was synthesized from compound **4** and purified according to the procedure described for **M7**. (Y = 60%). $^1\text{H-NMR}$ (500 MHz, CDCl_3) δ (ppm): 8.99 (s, 2H), 8.16 (s, 2H), 4.03–4.00 (m, 4H), 1.70–1.68 (m, 4H), 1.40–1.25 (m, 36H), 0.88–0.86 (m, 6H). $^{13}\text{C-NMR}$ (126 MHz, CDCl_3) δ (ppm): 160.8, 138.8, 138.4, 135.3, 131.3, 114.1, 112.7, 109.0, 42.4, 32.0, 30.1, 29.6, 29.4, 29.3, 26.9, 22.8, 14.2. m.p. = 230 °C. FTIR ν (cm^{-1}) = 3088, 2919, 2850, 2236, 1674, 1559, 884. HRMS (APPI+): m/z calcd for $\text{C}_{40}\text{H}_{55}\text{N}_4\text{O}_2\text{S}_2$: 687.3766; found: 687.3775 $[\text{M} + \text{H}]^+$.

3.2.7. Synthesis of 3,6-(4-Cyano-thiophen-2-yl)-2,5-bis(2-decyltetradecyl)-pyrrolo[3,4-c]pyrrole-1,4-dione (**M9**)

M9 was synthesized from compound **4** and purified according to the procedure described for **M7** and **M8**. (Y = 52%). $^1\text{H-NMR}$ (400 MHz, CDCl_3) δ (ppm): 8.91 (d, $J = 1.2$ Hz, 2H), 8.15 (d, $J = 1.2$ Hz, 2H), 3.95 (d, $J = 7.7$ Hz, 4H), 1.78(br, 2H), 1.39–1.09 (m, 80H), 0.96–0.78 (m, 12H). $^{13}\text{C-NMR}$ (101 MHz, CDCl_3) δ (ppm): 161.1, 139.0, 138.1, 135.1, 131.2, 113.9, 112.4, 109.0, 46.3, 31.9, 29.9, 29.7, 29.6, 29.5, 26.2, 22.6, 14.1. HRMS (APPI+): m/z calcd for $\text{C}_{63}\text{H}_{103}\text{N}_4\text{O}_2\text{S}_2$: 1023.7522; found: 1023.7546 $[\text{M} + \text{H}]^+$.

3.2.8. Synthesis of **P3**

M1 (0.076 mmol, 1 eq.), **M8** (0.076 mmol, 1 eq.), *trans*-bis(acetato)bis[*o*-(di-*o*-tolylphosphino)benzyl]dipalladium (II) (2% mol), tris(2-methoxyphenyl)phosphine (8% mol), Cs_2CO_3 (3 eq.) and pivalic acid (1 eq.) were put in a microwave vial with a magnetic stirring bar. The vial was sealed with a cap and then purged with nitrogen to remove the oxygen (3X). Degassed and anhydrous toluene was added ($C = 0.2 \text{ mol}\cdot\text{L}^{-1}$, 0.4 mL) and the microwave vial was heated at 120 °C using a slow temperature ramp. After heating for 5 min, gelation of the reaction mixture occurred and the reaction was stopped. Chloroform was added to solubilize the mixture (2 mL) and then the mixture was poured in methanol/acidified water (10% HCl; 9:1 ratio), and the solid was recovered by filtration using a 0.45 μm nylon filter. The polymer was washed using a Soxhlet apparatus with acetone, hexanes, then chloroform. The chloroform fraction was reduced to 5–10 mL and then poured in methanol. The polymer was recovered by filtration over a 0.45 μm nylon filter and dried under vacuum (Y = 65%).

3.2.9. Synthesis of **P6**

M2 (0.12 mmol, 1 eq.), **M7** (0.12 mmol, 1 eq.), $\text{Pd}(\text{OAc})_2$ (4% mol), tris(2-cycloheptyloxyphenyl)phosphine (BuraPhos) (16% mol), Cs_2CO_3 (3 eq.) and pivalic acid (1 eq.) were put in a microwave vial with a magnetic stirring bar. The vial was sealed with a cap and then purged with nitrogen to remove the oxygen (3X). Degassed and anhydrous THF was added ($C = 0.1 \text{ mol}\cdot\text{L}^{-1}$, 1.2 mL) and the reaction was heated with an oil bath pre-heated at 100 °C (reaction under pressure) until gelation of the reaction mixture. After 40 min, gelation of the reaction mixture occurred and the reaction was stopped. The reaction was cooled to 65 °C and then 2 mL of ODCB was added and the mixture was heated at 100 °C for 5 min. The mixture was poured in methanol/acidified water (10% HCl; 9:1 ratio), and the solid was recovered by filtration using a 0.45 μm nylon filter. The polymer was washed using a Soxhlet apparatus with acetone, hexane, and then chlorobenzene.

The chlorobenzene fraction was reduced to 5–10 mL and then poured in methanol. The polymer was recovered by filtration over a 0.45 μm nylon filter and dried under vacuum ($Y = 80\%$).

3.2.10. Synthesis of **P7a**

M9 (0.143 mmol, 1 eq.), **M7** (0.143 mmol, 1 eq.), $\text{Pd}(\text{OAc})_2$ (4% mol), tris(2-cycloheptyloxyphenyl)phosphine (BuraPhos) (16% mol), Cs_2CO_3 (3 eq.) and pivalic acid (1 eq.) were put in a microwave vial with a magnetic stirring bar. The vial was sealed with a cap and then purged with nitrogen to remove the oxygen (3X). Degassed and anhydrous THF was added ($C = 0.085 \text{ mol}\cdot\text{L}^{-1}$, 1.7 mL) and the reaction was heated with an oil bath pre-heated at 100 $^\circ\text{C}$ (reaction under pressure). After 4h the reaction was stopped. The reaction was cooled to 65 $^\circ\text{C}$ and then 2 mL of ODCB was added and the mixture was heated at 100 $^\circ\text{C}$ for 5 min. The mixture was poured in methanol/acidified water (10% HCl; 9:1 ratio), and the solid was recovered by filtration using a 0.45 μm nylon filter. The polymer was washed using a Soxhlet apparatus with acetone and hexanes. The hexanes fraction was reduced to 5–10 mL and then poured in methanol. The polymer was recovered by filtration over a 0.45 μm nylon filter and dried under vacuum ($Y = 75\%$).

3.2.11. Synthesis of **P7b**

M9 (0.13 mmol, 1 eq.), **M7** (0.13 mmol, 1 eq.), $\text{Pd}(\text{OAc})_2$ (4% mol), tris(2-cycloheptyloxyphenyl)phosphine (BuraPhos) (16% mol), Cs_2CO_3 (3 eq.) and pivalic acid (1 eq.) were put in a microwave vial with a magnetic stirring bar. The vial was sealed with a cap and then purged with nitrogen to remove the oxygen (3X). Degassed and anhydrous THF was added ($C = 0.15 \text{ mol}\cdot\text{L}^{-1}$, 0.9 mL) and the reaction was heated with an oil bath pre-heated at 100 $^\circ\text{C}$ (reaction under pressure) until gelation of the reaction mixture. After 40 min, gelation of the reaction mixture occurred and the reaction was stopped. The reaction was cooled to 65 $^\circ\text{C}$ and then 2 mL of ODCB was added and the mixture was heated at 100 $^\circ\text{C}$ for 5 min. The mixture was poured in methanol/acidified water (10% HCl; 9:1 ratio), and the solid was recovered by filtration using a 0.45 μm nylon filter. The polymer was washed using a Soxhlet apparatus with acetone, hexanes and chloroform. The chloroform fraction was reduced to 5–10 mL and then poured in methanol. The polymer was recovered by filtration over a 0.45 μm nylon filter and dried under vacuum ($Y = 80\%$).

3.2.12. Synthesis of **P7c**

M9 (0.143 mmol, 1 eq.), **M7** (0.143 mmol, 1 eq.), $\text{Pd}(\text{OAc})_2$ (4% mol), tris(2-cycloheptyloxyphenyl)phosphine (BuraPhos) (16% mol), Cs_2CO_3 (3 eq.) and pivalic acid (1 eq.) were put in a microwave vial with a magnetic stirring bar. The vial was sealed with a cap and then purged with nitrogen to remove the oxygen (3X). Degassed and anhydrous Chlorobenzene was added ($C = 0.1 \text{ mol}\cdot\text{L}^{-1}$, 1.4 mL) and the reaction was heated with an oil bath pre-heated at 130 $^\circ\text{C}$ (reaction under pressure). After 24h the reaction was stopped. The reaction was cooled to 65 $^\circ\text{C}$ was poured in methanol/acidified water (10% HCl; 9:1 ratio), and the solid was recovered by filtration using a 0.45 μm nylon filter. The polymer was washed using a Soxhlet apparatus using acetone and only oligomers were recovered.

4. Conclusions

We have performed theoretical calculations on new electron-rich and electron-poor compounds for applications in organic electronics. These results led to the design and synthesis of new cyanated dithienyl-diketopyrrolopyrrole units (CNDT-DPP) that were suitable for the direct heteroarylation polymerization. Two classes of cyanated dithienyl-DPP-based copolymers (pseudo-homopolymer (**P3**) and push/pull copolymer (**P6**)) have been prepared and characterized. Upon cyanation, a strong stabilization of the LUMO energy level was observed for **P3** and **P6**. Based on their promising electro-optical properties, **P3** is currently tested as *n*-type material in OFETs and as an electron-acceptor

for the development of all-polymer solar cells while **P6** is currently tested as an electron-donating material in OSCs.

Supplementary Materials: The following are available online, Figures S1–S13 ^1H and ^{13}C -NMR spectra, Figures S14–S17 Infrared spectra and Figures S18–S20 GPC chromatogram.

Author Contributions: T.B. and S.B. synthesized and characterized all the monomers and polymers. M.-A.L. performed theoretical calculations. O.A.I. and N.L. help characterizing polymers. M.L. supervised the project.

Funding: NSERC Discovery Grant and Apogée Sentinelle Nord Grant.

Acknowledgments: The authors acknowledge the Natural Sciences and Engineering Research Council of Canada (NSERC) and Université Laval (APOGÉE, Sentinelle Nord). Compute Canada and Calcul Québec are also thanked for access to computational facilities. The authors also thank Yuning Li (University of Waterloo, Ontario, CANADA) for useful discussions.

Conflicts of Interest: The authors declare no conflict of interest.

References

1. Lu, L.; Zheng, T.; Wu, Q.; Schneider, A.M.; Zhao, D.; Yu, L. Recent advances in bulk heterojunction polymer solar cells. *Chem. Rev.* **2015**, *115*, 12666–12731. [[CrossRef](#)] [[PubMed](#)]
2. Etxebarria, I.; Ajuria, J.; Pacios, R. Solution-processable polymeric solar cells: A review on materials, strategies and cell architectures to overcome 10%. *Org. Electron.* **2015**, *19*, 34–60. [[CrossRef](#)]
3. Sondergaard, R.; Hösel, M.; Angmo, D.; Larsen-Olsen, T.T.; Krebs, F.C. Roll-to-roll fabrication of polymer solar cells. *Mater. Today* **2012**, *15*, 36–49. [[CrossRef](#)]
4. Hösel, M.; Dam, H.F.; Krebs, F.C. Development of lab-to-fab production equipment across several length scales for printed energy technologies, including solar cells. *Energy Tech.* **2015**, *3*, 293–301. [[CrossRef](#)]
5. Tsai, P.T.; Tsai, C.Y.; Wang, C.M.; Chang, Y.F.; Meng, H.F.; Chen, Z.K.; Lin, H.W.; Zan, H.W.; Horng, S.F.; Lai, Y.C.; et al. High-efficiency polymer solar cells by blade coating in chlorine-free solvents. *Org. Electron.* **2014**, *15*, 893–903. [[CrossRef](#)]
6. Berny, S.; Blouin, N.; Distler, A.; Egelhaaf, H.J.; Krompiec, M.; Lohr, A.; Lozman, O.R.; Morse, G.E.; Nanson, L.; Pron, A.; et al. Solar trees: First large-scale demonstration of fully solution coated, semitransparent, flexible organic photovoltaic modules. *Adv. Sci.* **2016**, *3*, 1500342. [[CrossRef](#)] [[PubMed](#)]
7. Zhang, S.; Ye, L.; Hou, J. Breaking the 10% Efficiency Barrier in Organic Photovoltaics: Morphology and device optimization of well-known PBDTTT polymers. *Adv. Energy Mater.* **2016**, *6*, 1502529. [[CrossRef](#)]
8. Ouyang, X.; Peng, R.; Ai, L.; Zhang, X.; Ge, Z. Efficient polymer solar cells employing a non-conjugated small electrolyte. *Nat. Photonics* **2015**, *9*, 520–524. [[CrossRef](#)]
9. Zhou, H.; Zhang, Y.; Mai, C.K.; Collins, S.D.; Bazan, G.C.; Nguyen, T.Q.; Heeger, A.J. Polymer homo-tandem solar cells with best efficiency of 11.3%. *Adv. Mater.* **2015**, *27*, 1767–1777. [[CrossRef](#)] [[PubMed](#)]
10. Zhao, W.; Li, S.; Yao, H.; Zhang, S.; Zhang, Y.; Yang, B.; Hou, J. Molecular optimization enables over 13% in organic solar cells. *J. Am. Chem. Soc.* **2017**, *139*, 7148–7151. [[CrossRef](#)] [[PubMed](#)]
11. Zhang, S.; Qin, Y.; Zhu, J.; Hou, J. Over 14% Efficiency in polymer solar cells enable by a chlorinated polymer donor. *Adv. Mater.* **2018**, *30*, 1800868. [[CrossRef](#)] [[PubMed](#)]
12. Kang, I.; Yun, H.J.; Chung, D.S.; Kwon, S.K.; Kim, Y.H. Record high hole mobility in polymer semiconductors via side-chain engineering. *J. Am. Chem. Soc.* **2013**, *135*, 14896–14899. [[CrossRef](#)] [[PubMed](#)]
13. Yun, H.J.; Kang, S.J.; Xu, Y.; Kim, S.O.; Kim, Y.H.; Noh, Y.Y.; Kwon, S.K. Dramatic inversion of charge polarity in Diketopyrrolopyrrole-based organic field-effect transistors via simple nitrile group substitution. *Adv. Mater.* **2014**, *26*, 7300–7307. [[CrossRef](#)] [[PubMed](#)]
14. Mercier, L.G.; Leclerc, M. Direct (Hetero)Arylation: A new tool for polymer chemists. *Acc. Chem. Res.* **2013**, *46*, 1597–1605. [[CrossRef](#)] [[PubMed](#)]
15. Bura, T.; Blaskovits, T.; Leclerc, M. Direct(hetero)arylation polymerization (DHAP): Trends and perspectives. *J. Am. Chem. Soc.* **2016**, *138*, 10056–10071. [[CrossRef](#)] [[PubMed](#)]
16. Pouliot, J.-R.; Grenier, F.; Blaskovits, T.; Beaupré, S.; Leclerc, M. Direct (Hetero)arylation polymerization: Simplicity for conjugated polymers synthesis. *Chem. Rev.* **2016**, *116*, 14225–14274. [[CrossRef](#)] [[PubMed](#)]
17. Nitti, A.; Po, R.; Bianchi, G.; Pasini, D. Direct Arylation strategies in the synthesis of n-extended monomers for organic polymeric solar cells. *Molecules* **2017**, *22*, 21. [[CrossRef](#)] [[PubMed](#)]

18. Hendsbee, A.; Li, Y. Performance Comparisons of polymer semiconductors synthesized by Direct (Hetero)Arylation Polymerization (DHAP) and conventional methods for organic thin film transistors and organic photovoltaics. *Molecules* **2018**, *23*, 1255. [[CrossRef](#)] [[PubMed](#)]
19. Gobalasingham, N.S.; Thompson, B.C. Direct Arylation Polymerization: A guide to optimal conditions for effective conjugated polymer. *Prog. Polym. Sci.* **2018**, *83*, 135–201. [[CrossRef](#)]
20. Nakabayashi, K. Direct Arylation Polycondensation as conjugated polymer synthesis methodology. *Polym. J.* **2018**, *50*, 475–483. [[CrossRef](#)]
21. Mercier, L.G.; Pron, A.; Leclerc, M. Direct Arylation/Heteroarylation Polycondensation Reaction. In *Conjugated Polymers: A Practical Guide to Synthesis*; RSC Publishing: Cambridge, UK, 2014; pp. 422–442.
22. Leclerc, M.; Beaupré, S. *Direct (Hetero)arylation Polymerization, Synthetic Methods for Conjugated Polymers and Carbon Materials*; Wiley-VCH Verlag GmbH & Co.: Weinheim, Germany, 2017; pp. 131–158.
23. Iizuka, E.; Wakioka, M.; Ozawa, F. Mixed-ligand approach to palladium-catalyzed direct arylation polymerization: Synthesis of donor-acceptor polymers with Dithienosilole (DTS) and Thienopyrroledione (TPD) units. *Macromolecules* **2015**, *48*, 2989–2993. [[CrossRef](#)]
24. Iizuka, E.; Wakioka, M.; Ozawa, F. Mixed-ligand approach to palladium-catalyzed Direct Arylation Polymerization: Effective prevention of structural defects using diamines. *Macromolecules* **2016**, *49*, 3310–3317. [[CrossRef](#)]
25. Wakioka, M.; Takahashi, R.; Ichihara, N.; Ozawa, F. Mixed-ligand approach to palladium-catalyzed Direct Arylation Polymerization: Highly selective synthesis of *n*-Conjugated polymers with Diketopyrrolopyrrole units. *Macromolecules* **2017**, *50*, 927–934. [[CrossRef](#)]
26. Bura, T.; Beaupré, S.; Ibraikulov, O.A.; Légaré, M.-A.; Quinn, J.; Lévêque, P.; Heiser, T.; Li, Y.; Leclerc, N.; Leclerc, M. New fluorinated dithienyl-diketopyrrolo-pyrrole monomers and polymers for organic electronics. *Macromolecules* **2017**, *50*, 7080–7090. [[CrossRef](#)]
27. Bura, T.; Beaupré, S.; Légaré, M.-A.; Quinn, J.; Rochette, E.; Blaskovits, J.T.; Fontaine, F.-G.; Pron, A.; Li, Y.; Leclerc, M. Direct Heteroarylation Polymerization: Guidelines for defect-free conjugated polymers. *Chem. Sci.* **2017**, *8*, 3913–3925. [[CrossRef](#)] [[PubMed](#)]
28. Choi, H.; Ko, S.J.; Kim, T.; Morin, P.O.; Walker, B.; Lee, B.H.; Leclerc, M.; Kim, J.Y.; Heeger, A.J. Small-bandgap polymer solar cells with unprecedented short-circuit current density and high fill factor. *Adv. Mater.* **2015**, *27*, 3318–3324. [[CrossRef](#)] [[PubMed](#)]
29. Li, J.; Zhao, Y.; Tan, H.S.; Guo, Y.; Di, C.A.; Yu, G.; Liu, Y.; Lin, M.; Lim, S.H.; Zhou, Y.; et al. A stable solution-processed polymer semiconductor with record high-mobility for printed transistors. *Sci. Rep.* **2012**, *2*, 754. [[CrossRef](#)] [[PubMed](#)]
30. Farnum, D.G.; Mehta, G.; Moore, G.G.I.; Siegel, F.P. Attempted reformatskii reaction of benzonitrile, 1,4-diketo-3,6-diphenylpyrrolo[3,4-c]pyrrole. A lactam analogue of pentalene. *Tetrahedron Lett.* **1974**, *15*, 2549–2552. [[CrossRef](#)]
31. Wallquist, O.; Lenz, R. 20 years of DPP pigments—Future perspectives. *Macromol. Symp.* **2002**, *187*, 617–629. [[CrossRef](#)]
32. Grzybowski, M.; Gryko, D.T. Diketopyrrolopyrrole: Synthesis, Reactivity, and Optical Properties. *Adv. Opt. Mater.* **2015**, *3*, 280–320. [[CrossRef](#)]
33. Yi, Z.; Wang, S.; Liu, Y. Design of high-mobility diketopyrrolopyrrole-based π -conjugated copolymers for organic thin-film transistors. *Adv. Mater.* **2015**, *27*, 3589–3606. [[CrossRef](#)] [[PubMed](#)]
34. Li, W.; Hendriks, K.H.; Wienk, M.M.; Janssen, R.A.J. Diketopyrrolopyrrole polymers for organic solar cells. *Acc. Chem. Res.* **2016**, *49*, 78–85. [[CrossRef](#)] [[PubMed](#)]
35. Dubnik, A.S.; Aldrich, T.J.; Eastham, N.D.; Chang, R.P.H.; Facchetti, A.; Marks, T.J. Tin-free direct C–H arylation polymerization for high photovoltaic efficiency conjugated copolymers. *J. Am. Chem. Soc.* **2016**, *48*, 15699–15709.
36. Nitti, A.; Signorile, M.; Boiocchi, M.; Bianchi, G.; Po, R. PBDTPD for plastic solar cells via Pd(PPh₃)₄-catalyzed direct(hetero)arylation polymerization. *J. Mater. Chem. A* **2016**, *4*, 17163–17170.
37. Greve, D.R.; Apperloo, J.J.; Janssen, R.A.J. Synthesis and characterisation of novel regioregular polythiophenes 2-tuning the redox properties. *Eur. J. Org. Chem.* **2001**, 3437–3443. [[CrossRef](#)]
38. Liu, M.S.; Jiang, X.; Liu, S.; Herguth, P.; Jen, A.K.-Y. Effect of cyano substituents on electron affinity and electron-transporting properties of conjugated polymers. *Macromolecules* **2002**, *35*, 3532–3538. [[CrossRef](#)]

39. Seri, M.; Bolognesi, M.; Chen, Z.; Lu, S.; Koopman, W.; Facchetti, A.; Muccini, M. Fine structural tuning of cyanated dithieno[3,2-b:2',3'-d]silole-oligothiophene copolymers: Synthesis, characterization, and photovoltaic response. *Macromolecules* **2013**, *46*, 6419–6430. [[CrossRef](#)]
40. Qiu, M.; Brandt, R.G.; Niu, Y.; Bao, X.; Yu, D.; Wang, N.; Han, L.; Yu, L.; Xia, S.; Yang, R. Theoretical study on the rational design of cyano-substituted P3HT materials for OSCs: Substitution effect on the improvement of photovoltaic performance. *J. Phys. Chem. C* **2015**, *119*, 8501–8511. [[CrossRef](#)]
41. Xiong, Y.; Qiao, X.; Li, H. Nitrile-substituted thienyl and phenyl units as building blocks for high performance n-type polymer semiconductors. *Polym. Chem.* **2015**, *6*, 6579–6584. [[CrossRef](#)]
42. Nakabayashi, K.; Otani, H.; Mori, H. Benzodithiophene-based low band-gap polymers with deep HOMO levels: synthesis, characterization, and photovoltaic performance. *Polym. J.* **2015**, *47*, 617–623. [[CrossRef](#)]
43. Kim, H.G.; Kim, M.; Clement, J.A.; Lee, J.; Shin, J.; Hwang, H.; Sin, D.H.; Cho, K. Energy level engineering of donor polymers via inductive and resonance effects for polymer solar cells: effects of cyano and alkoxy substituents. *Chem. Mater.* **2015**, *27*, 6858–6868. [[CrossRef](#)]
44. Casey, A.; Han, Y.; Fei, Z.; White, A.J.P.; Anthopoulos, T.D.; Heeney, M. Cyano substituted benzothiadiazole: a novel acceptor inducing n-type behaviour in conjugated polymers. *J. Mater. Chem. C* **2015**, *3*, 265–275. [[CrossRef](#)]
45. Casey, A.; Dimitrov, S.D.; Shakya-Tuladhar, P.; Fei, Z.; Nguyen, M.; Han, Y.; Anthopoulos, T.D.; Durrant, J.R.; Heeney, M. Effect of systematically tuning conjugated donor polymer lowest unoccupied molecular orbital levels via cyano substitution on organic photovoltaic device performance. *Chem. Mater.* **2016**, *28*, 5110–5120. [[CrossRef](#)]
46. Casey, A.; Green, J.P.; Shakya Tuladhar, P.; Kirkus, M.; Han, Y.; Anthopoulos, T.D.; Heeney, M. Cyano substituted benzotriazole based polymers for use in organic solar cells. *J. Mater. Chem. A* **2017**, *5*, 6465–6470. [[CrossRef](#)]
47. Heuvel, R.; van Franeker, J.J.; Janssen, R.A.J. Energy level tuning of poly(phenylene-*alt*-dithienobenzothiadiazole)s for low photon energy loss solar cells. *Macromol. Chem. Phys.* **2017**, *218*, 1600502. [[CrossRef](#)] [[PubMed](#)]
48. Liu, X.; Li, M.; He, R.; Shen, W. Theoretical investigations on fluorinated and cyano copolymers for improvements of photovoltaic performances. *Phys. Chem. Chem. Phys.* **2014**, *16*, 311–323. [[CrossRef](#)] [[PubMed](#)]
49. Suraru, S.-L.; Zschieschang, U.; Klauk, H.; Würthner, F. Diketopyrrolopyrrole as a p-channel organic semiconductor for high performance OTFTs. *Chem. Commun.* **2011**, *47*, 1767–1769. [[CrossRef](#)] [[PubMed](#)]
50. Zhao, Z.-W.; Pan, Q.-Q.; Li, S.-B.; Duan, Y.-A.; Geng, Y.; Zhang, M.; Su, Z.-M. A theoretical exploration of the effect of fluorine and cyano substitutions in diketopyrrolopyrrole-based polymer donor for organic solar cells. *J. Mol. Graph.* **2017**, *77*, 9–16. [[CrossRef](#)] [[PubMed](#)]
51. Roy, C.; Bura, T.; Beaupré, S.; Légaré, M.-A.; Sun, J.-P.; Hill, I.G.; Leclerc, M. Fluorinated Thiophene-Based Synthons: Polymerization of 1,4-dialkoxybenzene and Fluoro-Dithieno-2,1,3-benzothiadiazole by Direct Heteroarylation. *Macromolecules* **2017**, *50*, 4658–4667. [[CrossRef](#)]
52. Gorelski, S.I. Origins of regioselectivity if the palladium-catalyzed (aromatic) C–H bond metalation-deprotonation. *Coord. Chem. Rev.* **2013**, *257*, 153–164. [[CrossRef](#)]
53. Guo, C.; Quinn, J.; Sun, B.; Li, Y. Dramatically different charge transport properties of bithienyl diketopyrrolopyrrole-bithiazole copolymers synthesized *via* two direct (hetero)arylation polymerization routes. *Polym. Chem.* **2016**, *7*, 4515–4524. [[CrossRef](#)]
54. Pouliot, J.R.; Sun, B.; Leduc, M.; Najari, A.; Li, Y.; Leclerc, M. A high mobility dpp-based polymer obtained via direct(hetero)arylation polymerization. *Polym. Chem.* **2015**, *6*, 278–282. [[CrossRef](#)]
55. Ha, J.S.; Kim, K.H.; Choi, D.H. 2,5-Bis(2-octyldodecyl)pyrrolo[3,4-c]pyrrole-1,4-(2*H*,5*H*)-dione-Based Donor–Acceptor Alternating Copolymer Bearing 5,5'-Di(thiophen-2-yl)-2,2'-biselenophene Exhibiting $1.5 \text{ cm}^2 \cdot \text{V}^{-1} \cdot \text{s}^{-1}$ Hole Mobility in Thin-Film Transistors. *J. Am. Chem. Soc.* **2011**, *133*, 10364–10367. [[CrossRef](#)] [[PubMed](#)]
56. Blouin, N.; Michaud, A.; Gendron, D.; Wakim, S.; Plesu, R.; Belletête, M.; Durocher, G.; Tao, Y.; Leclerc, M. Towards a Rational Design of Poly(2,7-carbazole) Derivatives for Solar Cells. *J. Am. Chem. Soc.* **2008**, *130*, 732–742. [[CrossRef](#)] [[PubMed](#)]
57. Zou, Y.; Gendron, D.; Aïch, B.R.; Najari, A.; Tao, Y.; Leclerc, M. A High-Mobility Low-Bandgap Poly(2,7-carbazole) Derivative for Photovoltaic Applications. *Macromolecules* **2009**, *42*, 2891–2894. [[CrossRef](#)]

58. Li, Y.; Singh, S.P.; Sonar, P. A High Mobility P-Type DPP-Thieno[3,2-b]thiophene Copolymer for Organic Thin-Film Transistors. *Adv. Mater.* **2010**, *22*, 4862–4866. [[CrossRef](#)] [[PubMed](#)]
59. Conwell, E. Primary Photoexcitations. In *Conjugated Polymers: Molecular Excitons Versus Semiconductor Band Model*; Sariciftci, N.S., Ed.; World Scientific: Singapore, 1997.
60. Zhu, Y.; Champion, R.D.; Jenekhe, S.A. conjugated donor–acceptor copolymer semiconductors with large intramolecular charge transfer: Synthesis, optical properties, electrochemistry, and field effect carrier mobility of thienopyrazine-based copolymers. *Macromolecules* **2006**, *39*, 8712–8719. [[CrossRef](#)]

Sample Availability: Samples of the compounds are not available from the authors.



© 2018 by the authors. Licensee MDPI, Basel, Switzerland. This article is an open access article distributed under the terms and conditions of the Creative Commons Attribution (CC BY) license (<http://creativecommons.org/licenses/by/4.0/>).